ChemComm

Cite this: *Chem. Commun.*, 2012, **48**, 11757–11759

www.rsc.org/chemcomm

COMMUNICATION

A highly selective turn-on near-infrared fluorescent probe for hydrogen sulfide detection and imaging in living cells†

Rui Wang, Fabiao Yu, Lingxin Chen,* Hao Chen, Linjie Wang and Weiwei Zhang

Received 22nd August 2012, Accepted 4th October 2012
DOI: 10.1039/c2cc36088h

We have described a turn-on near-infrared fluorescent probe Cy–NO_2 based on nitro group reduction for intracellular H_2S detection. The probe employs cyanine dye as a fluorophore, and is equipped with a nitro group as a fluorescent modulator. It is readily employed for assessing intracellular H_2S level changes, and confocal imaging is achieved successfully.

Hydrogen sulfide (H_2S) is well known for its unpleasant rotten egg smell, which was considered as a toxic gas for a long time. However, many studies on endogenous H_2S have demonstrated that hydrogen sulfide is the most recent endogenous gasotransmitter along with nitric oxide (NO) and carbon monoxide (CO).[1] Endogenous hydrogen sulfide is biosynthesized by at least three separate enzymes: cystathionine-β-synthase (CBS),[2] cystathionine-γ-lyase (CSE),[3] and 3-mercaptopyruvate sulfurtransferase (3-MST).[4] It is reported that mitochondrial sulfide quinone oxidoreductase (SQR) and persulfide dioxygenase (SDO) are involved in the consumption of H_2S.[5] H_2S also appears to regulate inflammation.[6] Furthermore, some research studies also have indicated that the hydrogen sulfide levels are related to Down syndrome and Alzheimer's disease.[7]

The interest in understanding the physiological and pathological functions of hydrogen sulfide has been increasing steadily. A number of sensitive and selective methods have been developed for the detection of H_2S including colorimetry,[8] electrochemical analysis,[9] and gas chromatography.[10] However, these techniques often require post-mortem processing and/or destruction of tissues or cells,[11] and are hence not suitable for the analysis of endogenous H_2S in real-time. Compared with these biological detection technologies, the fluorescence method provides greater sensitivity, less invasiveness, and more convenience, and offers high sensitivity as well as real-time imaging.[12] Recently, there has been an explosive increase in the number of fluorescent probes for H_2S.[13] In general, these probes are divided into three types: exploiting a unique reduction reaction between an azide group and H_2S;[13a–c,15c] taking advantage of the double nucleophilic character of H_2S; utilizing a copper-centered coordination complex in which Cu^{2+} can be released by binding H_2S. However, most of these fluorescent probes emit in the ultraviolet or the visible region, which can be interfered by cell autofluorescence easily. In contrast, long wavelength probes with emission in the near-infrared (NIR) region are optimal for biological imaging applications due to minimal photo damage to biological samples and minimum interference from background auto-fluorescence in living systems.[14] Therefore, it is necessary to develop new types of fluorescent probes that can be used for H_2S detection under physiological conditions, preferably with emission located in the NIR region. On the other hand, it is reported that the nitro group can be reduced by Na_2S to produce the corresponding amino group under mild conditions,[15] which inspires us to design and synthesize a new type of fluorescent probe containing a nitro group for H_2S detection in cells. Herein, we present a new NIR fluorescent probe Cy–NO_2 for detection of H_2S in living cells.

As an overall strategy, the heptamethine cyanine was particularly chosen as a fluorophore, because of its high molar absorption coefficient and NIR emission, along with other members of the cyanine family, which have been used for a variety of fluorescence sensing applications. It is speculated that the fluorescence properties of the heptamethine cyanine dye could be modulated *via* a photo-induced electron transfer (PET) process from the excited fluorophore to a strong electron-withdrawing group (donor-excited PET; d-PET).[16] Therefore, *m*-nitrophenol was selected as a modulator for the Cy–NO_2 probe. After being equipped with *m*-nitrophenol, the fluorescence of the cyanine platform was quenched by the electron transfer process between the modulator and the fluorophore. As expected, the nitro group could be reduced to the amino group under physiological conditions, triggering an increase in the fluorescence emission, thereby allowing the formation of a "turn-on" fluorescent probe for H_2S detection. The structure and the proposed mechanism of fluorescence probe Cy–NO_2 for H_2S detection are shown in Scheme 1.

To verify whether the probe was suitable for the physiological detection, we evaluated the effect of pH on the fluorescence of the probe.[17] As shown in Fig. S1 (ESI†), the pH of the medium had hardly any effect on the fluorescence of Cy–NO_2 and its reduced product Cy–NH_2 over the pH range of 4.2–8.2. Therefore, the probe was expected to work well under physiological conditions (40 mM HEPES, pH 7.4).

The absorption and fluorescence spectra of the probe were examined under simulated physiological conditions (40 mM HEPES, pH 7.4, 10 μM Cy–NO_2). In the absence of H_2S,

Key Laboratory of Coastal Zone Environmental Processes, Yantai Institute of Coastal Zone Research, Chinese Academy of Sciences, Yantai 264003, P. R. China. E-mail: lxchen@yic.ac.cn; Fax: +86 535-2109130

† Electronic supplementary information (ESI) available: General methods, synthesis and characterization of compounds, effect of pH and temperature, MTT and bright-field confocal images. See DOI: 10.1039/c2cc36088h

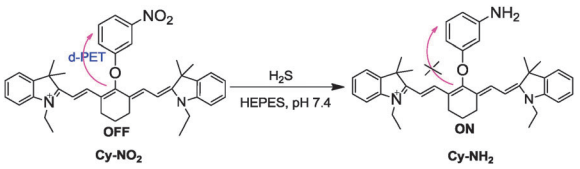

Scheme 1 Structures of Cy–NO_2, and its reduced product Cy–NH_2, and the proposed mechanism of fluorescence probe Cy–NO_2 for H_2S detection.

Cy–NO_2 exhibited λ_{max} for absorption and emission at 755 nm and 809 nm, respectively, both of which lie in the NIR region (Fig. 1). There is a significant decrease in the absorption spectrum upon addition of H_2S (Fig. 1a). We attributed the phenomenon of absorption decrease to the difference of molar absorptivity between Cy–NO_2 and Cy–NH_2. We calculated that the molar absorptivity of Cy–NH_2 ($\varepsilon_{755nm} = 3.4 \times 10^4\ M^{-1}\ cm^{-1}$) was much lower than that of Cy–NO_2 ($\varepsilon_{755nm} = 8.1 \times 10^4\ M^{-1}\ cm^{-1}$). Therefore, the absorption spectrum shows a significant decrease after addition of H_2S. Upon addition of different concentrations of H_2S to the buffer solution which contained 10 μM Cy–NO_2, the fluorescence intensity increased by ~12.7 fold and the quantum yield increased from 0.05 to 0.11. Interestingly, the emission spectrum showed little blue shift in λ_{max} from 809 nm to 789 nm (Fig. 1b). This phenomenon was induced by the push–pull electronic effect of the functional moiety.[18] Upon reduction by H_2S, the probe contained an electron-donating group (Ph–NH_2 moiety) instead of an electron-withdrawing group (Ph–NO_2 moiety). Therefore, the fluorescence spectrum underwent a slight blue shift.

During the experiments, interestingly, we found that the reaction rate between Cy–NO_2 and H_2S was severely affected by the reaction temperature. In order to optimize the reaction temperature, we tested the effect of temperature on the reaction rate. The probe (10 μM) and 350 μM Na_2S were equilibrated at different temperatures, and the fluorescence intensity was acquired in 40 mM HEPES (pH 7.4) with emission at 789 nm. As shown in Fig. S2 (ESI†), the reaction was very slow at room temperature. The fluorescence intensity could reach saturation within 40 min at 60 °C, but the temperature was too high to detect H_2S in living cells. Excitedly, the probe exhibited almost the same reaction rate under 37 °C and 45 °C conditions. The fluorescence intensity could reach saturation within 60 min. Thus, 37 °C was chosen as the optimal reaction temperature.

To verify whether there is fluorescence response to other biological analytes or not, Cy–NO_2 (10 μM) was treated with various biologically relevant analytes in HEPES buffer (40 mM, pH 7.4). Overall 24 biological species were screened. As shown in Fig. 2, Cy–NO_2 showed selective response for

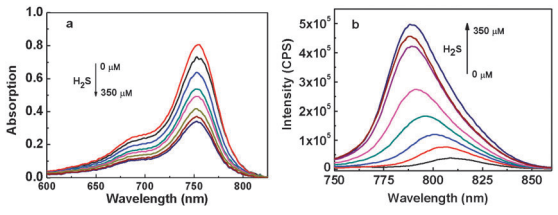

Fig. 1 (a) Absorption and (b) fluorescence spectra of probe Cy–NO_2 (10 μM) treated with various concentrations of H_2S: 0, 50, 100, 150, 200, 250, 300, 350 μM. Spectra were acquired in 40 mM HEPES, pH 7.4, at 37 °C after incubation of the probe with H_2S for 60 min with excitation at 755 nm and emission ranging from 755 to 900 nm.

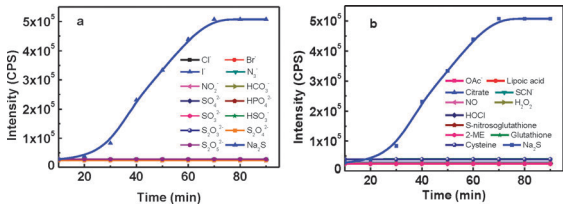

Fig. 2 Fluorescence responses and time courses of 10 μM Cy–NO_2 to biologically relevant species for 90 min. (a) Anions and RSS. (b) RNS and ROS. Data shown: Na_2S, HSO_3^-, SO_3^{2-}, $S_2O_3^{2-}$, $S_2O_4^{2-}$, $S_2O_5^{2-}$, NO, H_2O_2 at 300 μM. Cl^-, Br^-, I^-, N_3^-, NO_2^-, OAc^-, lipoic acid, citrate, glutathione, cysteine, *S*-nitrosoglutathione and 2-mercaptoethanol (2-ME) at 1 mM.

H_2S over reactive oxygen species (ROS), reactive nitrogen species (RNS) and anions. Of all the tested reactive sulfide species (RSS), only $S_2O_3^-$, $S_2O_4^{2-}$, $S_2O_5^{2-}$, glutathione and cysteine gave a limited increase in the fluorescence intensity. However, the intensity of the fluorescence increase was far weaker than that caused by H_2S. To check whether the probe might turn on fluorescence upon incubation with other biological species over time, the probe's time courses with various species for 90 min were measured. As demonstrated in Fig. 2, Cy–NO_2 can selectively respond to H_2S and avoid the interference of other relevant species. The experimental results displayed that the selective reduction of Cy–NO_2 to Cy–NH_2 could be used for the detection of H_2S under simulated physiological conditions.

We explored the ability of the probe to quantify H_2S in buffer solution and fetal bovine serum sample. To evaluate the ability of Cy–NO_2 in the detection of H_2S concentration, the probe was treated with different concentrations of H_2S (0–350 μM). The final concentration of the probe was maintained at 10 μM. For the purpose of accurate analysis, a linear relationship is always necessary. Herein, we obtained a calibration curve between fluorescence emission intensity and H_2S concentration. As shown in Fig. 3, the fluorescence signal was linearly related to the concentration of H_2S in the given concentration range. The regression equation was $F_{789nm} = 1111 \times [H_2S] + 19\,632$, with $r = 0.992$. Next, we used fetal bovine serum to investigate whether our probe could detect H_2S in complex biological samples. We prepared the fetal bovine serum samples containing H_2S in different concentrations (0–350 μM). Following the above method, we got another calibration curve between fluorescence emission intensity and H_2S concentration. The regression equation was $F_{789nm} = 1073 \times [H_2S] + 18\,012$, with $r = 0.996$. These results indicated that Cy–NO_2 could

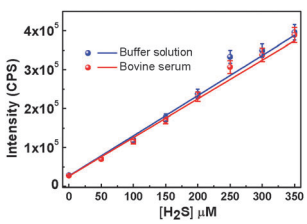

Fig. 3 The relationship between fluorescence intensity and H_2S concentration in buffer solution (40 mM HEPES, pH 7.4) (blue) and commercial fetal bovine serum (red). The concentration of fetal bovine serum in the solution is 15% (v/v). 10 μM Cy–NO_2 and H_2S 0–350 μM. The fluorescence intensity was acquired at 37 °C after incubation of the probe with H_2S for 60 min ($\lambda_{ex} = 755$ nm, $\lambda_{em} = 789$ nm).

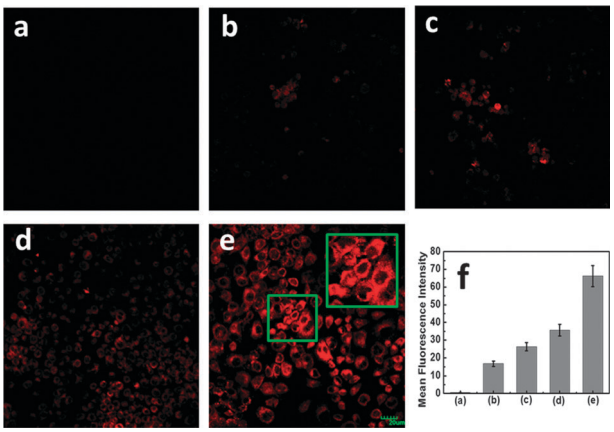

Fig. 4 Confocal fluorescence images of living RAW264.7 cells incubated with various concentrations of Na_2S. RAW264.7 cells loaded with 10 μM Cy–NO_2 and Na_2S for 30 min. (a) Control, (b) 50 μM, (c) 150 μM, (d) 250 μM, and (e) 350 μM Na_2S. Scale bar is 20 μm. Incubation was performed at 37 °C under a humidified atmosphere containing 5% CO_2. The fluorescence was collected at 650–800 nm upon excitation at 635 nm. (f) The relationship between average fluorescence intensity and added various Na_2S concentrations in a–e correspondingly. The cell body regions in the visual field (a–e) were selected as the regions of interest (ROI), and the average fluorescence intensity was determined *via* confocal laser-scanning microscopy. Data were normalized to controls and statistical analyses were performed with a two-tailed Student's *t*-test. $^*P < 0.05$ ($n = 3$). Error bars are ± s.e.m.

qualitatively and quantitatively detect H_2S in complex biological systems.

Having demonstrated the selectivity and sensitivity of Cy–NO_2 for H_2S *in vitro*, we next established the ability of Cy–NO_2 to track H_2S level changes in living cells by using a RAW264.7 cell model. RAW264.7 cells were incubated with 10 μM Cy–NO_2 for 10 min at 37 °C, and then washed with physiological saline to remove excess Cy–NO_2. The treated cells were incubated with buffer containing different concentrations of Na_2S (50, 150, 250 and 350 μM). After incubation for 30 min in RPMI 1640 Medium at 37 °C, the cells were washed with physiological saline to remove the excess Na_2S, and then the cells were imaged by a confocal fluorescence microscope. The fluorescence was collected at 650–800 nm upon excitation at 635 nm. As a control, the cells not treated with Na_2S were also imaged. The control experiments showed faint fluorescence (Fig. 4a), but those treated with various concentrations of Na_2S displayed different fluorescence intensities. The confocal fluorescence images grew brighter as the concentrations of Na_2S increased from 50 to 350 μM (Fig. 4b–e). The cell body regions in the visual field (Fig. 4a–e) were selected as the regions of interest (ROI), and the average fluorescence intensity was determined *via* confocal laser-scanning microscopy with various H_2S concentrations (Fig. 4f). The results suggested that Cy–NO_2 had good membrane permeability, and these data also established that Cy–NO_2 could respond to intracellular H_2S level changes within living cells.

We also applied Cy–NO_2 to the subcellular locations of H_2S in the RAW264.7 cells using confocal fluorescence microscopy. The cells, with the same condition used in Fig. 4e, were co-stained with Cy–NO_2 (10 μM) and Janus Green B (JGB, 1 μM) for 15 min. Fig. S5 (ESI†) further reveals the location of the probe in the cytoplasm of these living RAW264.7 cells. We also employed the Pearson correlation coefficient (r) which was used to quantify the degree of colocalization between fluorophores[19] to further reveal the subcellular locations of Cy–NO_2. By using Olympus software, we obtained the value of Cy–NO_2 with JGB $r = 0.85$, revealing that Cy–NO_2 primarily locates in the cytoplasm.

In summary, we have developed a new NIR fluorescent probe that exhibits high selectivity and sensitivity for H_2S both in aqueous solution and living cells. Our probe Cy–NO_2 shows remarkable turn-on fluorescence for H_2S compared to other biologically relevant species. Confocal microscopy images indicate that our probe can detect the level changes of H_2S in living cells. We anticipate that the fluorescent probe will be of great benefit for biomedical researchers to investigate the effects of H_2S in biological systems.

This work was financially supported by the National Natural Science Foundation of China (21275158, 31200041), the Innovation Projects of the Chinese Academy of Sciences (KZCX2-EW-206), and the 100 Talents Program of the Chinese Academy of Sciences.

Notes and references

1 (*a*) R. Wang, *Antioxid. Redox Signaling*, 2003, **5**, 493; (*b*) T. W. Miller, J. S. Isenberg and D. D. Roberts, *Chem. Rev.*, 2009, **109**, 3099.
2 (*a*) J. E. Dominy and M. H. Stipanuk, *Nutr. Rev.*, 2004, **62**, 348; (*b*) S. Singh, D. Padovani, R. A. Leslie, T. Chiku and R. Banerjee, *J. Biol. Chem.*, 2009, **284**, 22457.
3 T. Chiku, D. Padovani, W. Zhu, S. Singh, V. Vitvitsky and R. Banerjee, *J. Biol. Chem.*, 2009, **284**, 22457.
4 N. Shibuya, M. Tanaka, M. Yoshida, Y. Ogasawara, T. Togawa, K. Ishii and H. Kimura, *Antioxid. Redox Signaling*, 2009, **111**, 703.
5 T. M. Hildebrandt and M. K. Grieshaber, *FEBS J.*, 2008, **275**, 3352.
6 K. Abe and H. Kimura, *J. Neurosci.*, 1996, **16**, 1066.
7 (*a*) K. Eto, T. Asada, K. Arima, T. Makifuchi and H. Kimura, *Biochem. Biophys. Res. Commun.*, 2002, **293**, 1485; (*b*) S. Fiorucci, E. Antonelli, A. Mencarelli, S. Orlandi, B. Renga, G. Rizzo, E. Distrutti, V. Shah and A. Morelli, *Hepatology*, 2005, **42**, 539; (*c*) G. D. Yang, L. Y. Wu, B. Jiang, W. Yang, J. S. Qi, K. Cao, Q. H. Meng, A. K. Mustafa, W. T. Mu, S. M. Zhang, S. H. Snyder and R. Wang, *Science*, 2008, **322**, 587.
8 M. G. Choi, S. Cha, H. Lee, H. L. Jeon and S. K. Chang, *Chem. Commun.*, 2009, 7390.
9 D. G. Searcy and M. A. Peterson, *Anal. Biochem.*, 2004, **324**, 269.
10 P. R. Brub, P. D. Parkinson and E. R. Hall, *J. Chromatogr., A*, 1999, **830**, 485.
11 (*a*) J. Furne, A. Saeed and M. D. Levitt, *Am. J. Physiol.*, 2008, **295**, R1479; (*b*) Y. Han, J. Qin, X. Chang, Z. Yang and J. Du, *Cell. Mol. Neurobiol.*, 2006, **26**, 101.
12 T. Ueno and T. Nagano, *Nat. Methods*, 2011, **8**, 642.
13 (*a*) A. R. Lippert, E. J. New and C. J. Chang, *J. Am. Chem. Soc.*, 2011, **133**, 10078; (*b*) H. Peng, Y. Cheng, C. Dai, A. L. King, B. L. Predmore, D. J. Lefer and B. Wang, *Angew. Chem., Int. Ed.*, 2011, **50**, 9672; (*c*) F. B. Yu, P. Li, P. Song, B. S. Wang, J. Z. Zhao and K. L. Han, *Chem. Commun.*, 2012, **48**, 2852; (*d*) Y. Qian, L. Zhang, S. Deng, X. Deng, C. He, H. Zhu and J. Zhao, *Chem. Sci.*, 2012, **3**, 2920, for more examples see ESI†.
14 R. Weissleder, *Nat. Biotechnol.*, 2001, **19**, 316.
15 (*a*) T. E. Nickson, *J. Org. Chem.*, 1986, **51**, 3903; (*b*) D. Huber, G. Andermann and G. Leclerc, *Tetrahedron Lett.*, 1988, **29**, 635; (*c*) L. A. Montoya and M. D. Pluth, *Chem. Commun.*, 2012, **48**, 4767.
16 T. Ueno, Y. Urano, H. Kojima and T. Nagano, *J. Am. Chem. Soc.*, 2006, **127**, 10640.
17 (*a*) A. Loudet and K. Burgess, *Chem. Rev.*, 2007, **107**, 4891; (*b*) R. Wang, C. Yu, F. Yu and L. Chen, *TrAC, Trends Anal. Chem.*, 2010, **29**, 1004.
18 K. Kiyose, S. Aizawa, E. Sasaki, H. Kojima, K. Hanaoka, T. Terai, Y. Urano and T. Nagano, *Chem.–Eur. J.*, 2009, **15**, 9191.
19 J. Adler and I. Parmryd, *Cytometry, Part A*, 2010, **77**, 733.